Communications: SIF Congress 2022

Radiobiological model for β-emitter radiopharmaceutical therapy in dynamic cell cultures in the framework of the ISOLPHARM project

Alberto Arzenton(^{1})(^{2})(*) on behalf of the ISOLPHARM Collaboration

(^{1}) *Dipartimento di Scienze Fisiche, della Terra e dell'Ambiente, Università di Siena - Siena, Italy*
(^{2}) *INFN, Laboratori Nazionali di Legnaro - Legnaro (PD), Italy*

Summary. — In medical physics and radiobiology, the most common method to probe the efficacy of radiation therapy approaches *in vitro* is the cell survival trial. Recently, the traditional procedure for external beams has been extended by some groups to targeted radionuclides. In parallel, the bioengineering state of the art allows for the use of 3D tissue-mimicking scaffolds to obtain realistic cell cultures in dynamic conditions. The aim of this study is to implement a mathematical model for the assessment of β-emitting radiopharmaceuticals, considering their molecular kinetics *in vitro* and how it affects the radiation delivery to cells. The molecular transitions will be assumed to fulfill the definition of Markov processes, while the cell survival will depend on the DNA damage, in competition with a logistic growth. The solutions of the resulting differential system will be evaluated by means of numerical examples. This work belongs to the framework of the ISOLPHARM project, headed by INFN-LNL, which has the aim of developing innovative radiopharmaceuticals exploiting the Isotope Separation On-Line (ISOL) at the SPES facility.

1. – Introduction

The mathematical modelling of the cellular response to ionizing radiation, namely the theoretical branch of radiobiology, is an enticing challenge that the biophysics and medical physics communities have been facing since the 1920s, even before the discovery of the DNA itself. The most common model nowadays is the Linear Quadratic (LQ), born in the late 1960s as an empirical model but then partially justified by theoretical

---

(*) E-mail: alberto.arzenton@lnl.infn.it

arguments. The model expresses the surviving fraction S of a cell population as a function of the absorbed dose D,

$$(1) \qquad\qquad S(D) = \exp\left(-aD - bD^2\right),$$

where the parameters a and b reflect the cell death caused by single and multiple hits. It is widely used in conventional radiotherapy planning, even though some weaknesses can be found in the low-dose regime ($D < 1\,\mathrm{Gy}$), where a region of hyper-radiosensitivity appears, followed by a subsequent window of increased radioresistance. [1-3]

In more recent times, the opportunity to exploit advanced Monte Carlo software, like GEANT4-DNA, PHITS and PARTRAC, has allowed for the development of mechanistic models directly investigating the DNA strand breaks at the molecular level, reproducing the geometry of the cell nucleus; such models are able to consider both the direct radiation damage on the DNA and the indirect damage acting through the formation of free radicals and reactive oxygen species in the cell environment [4-11]. A state-of-the-art experimental feedback to this kind of models is given by the γ-H2AX assay, which enables the visualization of the DNA Double Strand Break (DSB) sites, the so-called *foci*, thanks to a specific fluorescent ligand; often, the DNA damage is computationally modeled with the definition of Complex Lesion (CL), occurring when a critical number of DSBs is reached within a critical distance [12-14]. Besides the computational approaches, advanced theoretical models managed to describe analytically the DNA damage probability, also considering that a single cell can undergo multiple CLs, and the repair pathways, finding good agreement with experimental data [15, 16].

Up to now, preclinical radiobiology has been mostly tailored in order to measure and assess the effects of external beams on cells and, as a consequence, radiation biophysics modeling has been moving in the same direction. However, some non-negligible differences emerge when switching to targeted radioisotopes.

1) The dose-rate per cell depends on the number of cell receptors that can bind the radioactive molecules, hence on the total number of living cells in the culture.

2) The ionizing radiation is not administered in uniform cycles, but it decays exponentially in time.

3) The exposure time is longer and, in general, comparable to the characteristic time of the biological processes affecting the cell population, namely DNA repair, cell growth and cell death.

It is clear that the amount of the cell population must be taken into account for the whole exposure time; for this reason, rather than expressing the cell survival as a function of the absorbed dose, it appears more interesting to consider the cell survival and the dose-rate per cell as functions of time, for a given administered activity [17, 18]. Recently, some groups have tried to develop new radiobiological protocols optimized for the *in vitro* testing of radiopharmaceuticals and, contextually, cell population models exploiting the definition of Markov processes for the description of the pharmacokinetic, physical and biological mechanisms began to be employed in this field [19-22]. Moreover, cellular dosimetry calculations have been related to several experiments in order to match the dose absorbed by the cell nucleus to the surviving fraction, usually applying the procedure suggested by the American committee on the Medical Internal Radiation Dose (MIRD), which is based on the S-values formalism [23-25].

Finally, from a purely biological point of view, the new frontiers in the experimental practice are characterized by more realistic 3D cell cultures obtainable thanks to innovative scaffolds made of tissue-mimicking materials, such as the hydrogel-based bioinks coming from the bioengineering *avant-garde*. Cells can be fed and grown to form bodily organoids or cancer spheroids, which permit to perform more advanced research *in vitro* and partially reduce the *in vivo* trials. 3D cultures can also be dynamic, which means that the cells can be placed in a bioreactor and fed continuously, mimicking the provision of nutrients managed by the blood circulation. [26, 27]

This work was conceived in the context of the ISOLPHARM project, which is headed by the Legnaro National Laboratories (LNL) of the Italian National Institute for Nuclear Physics (INFN); its purpose is the development of innovative radiopharmaceuticals exploiting the nuclides produced by the Isotope Separation On-Line (ISOL) technique at the SPES facility, currently under construction. ISOLPHARM relies on a strong national collaboration involving also the INFN sections of Padova, Pavia, Trento, Bologna and Pisa (Siena division), as well as the Southern National Laboratories (LNS), and the universities of Padova, Pavia, Trento, Bologna, Siena, Catania and Brescia. A similar network has favoured the interaction between researchers with different expertise, from physics and chemistry to biology and pharmacology, in order to carry out interdisciplinary activities in the INFN experiments ISOLPHARM_Ag (2018–2019) and ISOLPHARM_EIRA (2020–2022) [28-33]. The present work is meant to be a pilot study for the third experiment promoted by the ISOLPHARM collaboration, ADMIRAL (2023–2025), whose purpose is to evaluate the therapeutic and diagnostic power of the β-emitter ^{111}Ag; in particular, a radiobiological experimental campaign will test the *in vitro* cellular response to ^{111}Ag-labeled drugs in conventional 2D and innovative 3D cell cultures. A theoretical support to those activities will be provided by computational simulations of cellular dosimetry and DNA damage; however, for the aforementioned reasons, the output of these simulations will need to be inserted in a proper cell population model before being compared to the cell survival data. This is indeed the purpose of the present work, which will try to implement a cell population model with a cumulative DNA damage mechanism and with the possibility to consider non-uniform activity distributions, like the ones that can be expected in 3D scaffolds.

2. – Model development

To build the model, several aspects must be taken into account. The first brick concerns the molecular kinetics, since knowing how much radiopharmaceutical is free or bound to the target receptors at time t is fundamental to proceed. Then, the result has to be matched to the equations regulating the cell population, which must also include a parameterization of the cell damage. Finally, a strategy to extend the resulting model also to the condition of non-uniform activity delivery in the culture will be studied.

In the mathematical modeling of biological and biophysical systems, it is common to employ the definition of Markov processes for any kind of transitions whose probability to happen in a given time interval does not depend on the history of the initial state. Following this formalism, a generic state i will undergo a transition towards another state j with a rate p, yielding, in a time window dt, a transition probability pdt (p has to be constant at least in dt). Considering a function $f(t)$ expressing the number of elements of a system in the state i, its variation $df(t)$ will be

$$(2) \qquad\qquad df(t) = -pf(t)dt,$$

which, in the $dt \to 0$ limit, gives $\dot{f}(t) = -pf(t)$. It is important to state, especially for computational reasons, that dt must be short enough to consider it improbable for a single element to undergo more than one transition in dt. The molecular kinetics and cell population equations will be built making use of these assumptions for several processes.

2.1. *Molecular kinetics*. – The first feature to analyze is the radiopharmaceutical uptake, namely its binding and unbinding processes to the cell receptors. Let us consider a drug that simply binds to a receptor on the cell membrane, without being internalized. This is a suitable condition for β-emitters, since their radiation range is sufficiently long to reach the cell nucleus, where the DNA is contained, while α and Auger emitters may not work properly. In this situation, the unbinding process will be simply regulated by a transition rate β, whereas the binding will be proportional to the number of available receptors with a constant α. In this way, the equations will include the receptor saturation effect: as a matter of fact, when a big fraction of the receptors has already been employed, it is more difficult for a free drug molecule to find an available site. Finally, in an *in vivo* system, a third rate γ would represent the biological elimination of the free drug by the excretory apparatus. Calling $x(t)$ and $y(t)$ the number of unbound and bound molecules, N_r the number of receptors per cell and $z(t)$ the number of cells,

$$(3) \qquad \begin{cases} \dot{x}(t) = -\alpha\big(N_r z(t) - y(t)\big)x(t) + \beta y(t) - \gamma x(t), \\ \dot{y}(t) = \alpha\big(N_r z(t) - y(t)\big)x(t) - \beta y(t), \end{cases}$$

where $N_r z(t) - y(t)$ clearly represents the number of available receptors; on the other hand, if the drug is internalized, the receptors are not occupied and the binding process could be described by a constant rate, just like the unbinding. However, this work focuses on *in vitro* practice, where $\gamma = 0$ and $y(t) = x_{in} - x(t)$ with $x_{in} \equiv x(0)$ ($t = 0$ is assumed as the injection time); hence, the system degenerates to a single equation,

$$(4) \qquad \dot{x}(t) = -\alpha\big(N_r z(t) - x_{in} + x(t)\big)x(t) + \beta\big(x_{in} - x(t)\big).$$

Numerical examples of eqs. (3) and (4) are shown in fig. 1, considering a fixed value for $z(t)$. It is clear that in a similar context $x(t)$ has an asymptotic equilibrium for $t \to +\infty$, which can be calculated setting $\dot{x}(t) = 0$ and considering only the positive solution,

$$(5) \qquad x_{eq}(z) = \frac{\sqrt{(N_r z - x_{in} + \beta/\alpha)^2 + 4x_{in}\beta/\alpha} - N_r z + x_{in} - \beta/\alpha}{2},$$

where the α and β rates appear only in the form β/α, meaning that experimentally it may not be necessary to measure both.

A few more words can be spent here for a better comprehension of the physical meaning of α, which may be defined as *single receptor binding rate*. It represents indeed the average binding rate of the drug to one particular receptor: if multiplied $N_r z(0)$ times, it gives the overall binding rate of the system when all the receptors are available[1]. α is not measurable but, since N_r and $z(0)$ should be known for the cell line under study,

---

[1] We are tacitly assuming that $z(0)$ is the maximum cell number containable by the culture.
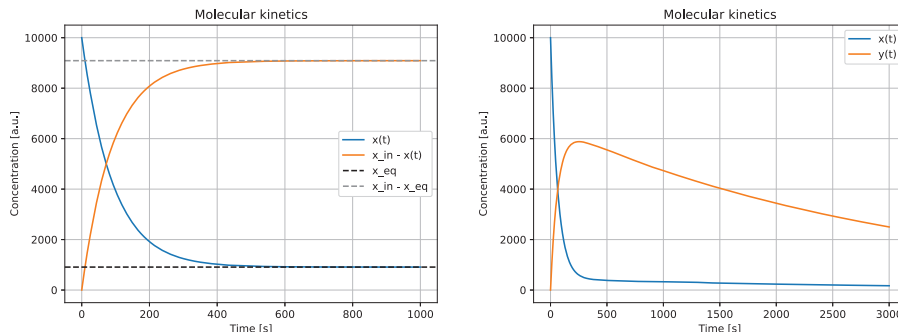
Fig. 1. – Left: molecular uptake kinetics of a radiopharmaceutical binding to the cell membrane *in vitro*, setting $\alpha = 10^{-3}\,\text{s}^{-1}$, $\beta = 10^3\,\text{s}^{-1}$, $N_\text{r} = 10^4$, $x_\text{in} = 10^4$, $z = 10^3$; right: *in vivo* case with the addition of $\gamma = 5 \times 10^{-3}\,\text{s}^{-1}$.

it could be obtained by a measurement of the overall rate right after the radiopharmaceutical injection, $\alpha N_\text{r} z(0^+)$, or using a stable isotope. Finally, for a fixed z, a constant rate $\alpha N_\text{r} z$ could be assumed in the $N_\text{r} z \gg x_\text{in}$ limit, as seen in eq. (4).

At this point, let us focus on the cell population, $z(t)$. Its behaviour will be studied better below, but we already know that the characteristic times of the processes affecting it may take several hours, while pharmacokinetics acts at smaller timescales [14,34]. As just shown, $x(t)$ has an asymptotic equilibrium when z is fixed; thus, if the uptake is much faster than the cell number variation, we can simplify our system by associating $x_\text{eq}(z)$ to every z. Naturally, this timescale separation is reliable only in presence of a highly performing targeting agent; such an approximation can be very helpful also from a computational point of view, since a bigger $\text{d}t$ can be chosen in the numerical analysis. Actually, the *in vitro* behavior expressed by eq. (4) represents a lucky case; for instance, eq. (3) reaches the equilibrium only when there is no more drug left, due to the effect of the biological elimination γ, typical of *in vivo* systems. For simplicity, from now on we will build our radiobiological model considering the timescale separation, thus using the $x_\text{eq}(z)$ defined by eq. (5). Anyway, we must remember that for slow uptake kinetics —which is undesirable for a therapeutic radiopharmaceutical— this approximation will not work and eq. (4) will have to be implemented in the final system.

2˙2. *Radiobiological assumptions*. – Let us now approach the description of the processes affecting the cell population, *i.e.*, DNA damage and repair, cell growth and cell death. The idea is to adopt the CL definition provided in sect. **1** and split the cell population into N compartments containing cells with increasing number of unrepaired CLs at time t. The notation used and the rules followed by the compartments can be summarized as follows (see also the scheme in fig. 2).

1) The n-th compartment, containing cells with n CLs at time t, is called $z_n(t)$, while $z(t)$ remains the total number of cells; $z_0(t)$ represents the undamaged cells, which are also the only ones considered capable of growing by mitosis.

2) An additional compartment, $z_\text{a}(t)$, includes the cells in which one or more CLs have degenerated into lethal aberrations, implying sure death with a rate η; such cells still express the target receptors, hence they contribute to the total amount $z(t)$.
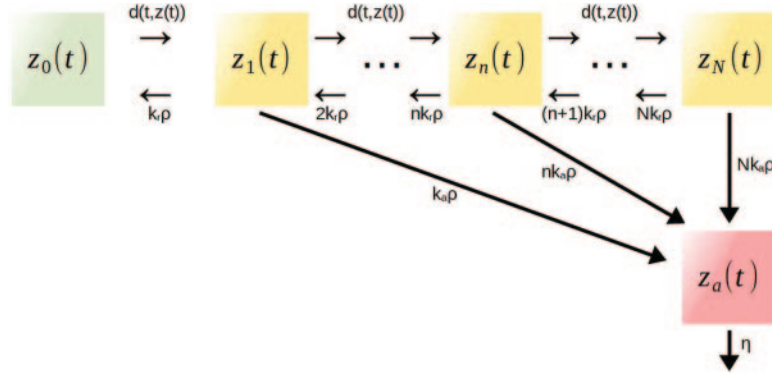
Fig. 2. – Illustrative scheme of the cellular compartments considered in the present model.

3) Each CL has a constant repair rate ρ, while the damage rate d depends on t and $z(t)$ and will be defined below; the CL can be successfully repaired with a probability $k_r \in [0, 1]$, otherwise it becomes a lethal aberration with $k_a \equiv 1 - k_r$.

The damage rate, which is in fact a CL rate, can be built in a way that favors its computational simulation by means of Monte Carlo codes tailored for radiation transport, like the ones mentioned in sect. **1**. Since the β radiation range is long with respect to the cell size, S-values can be computed to identify the average CL rate for a decay event coming from the cell membrane, from neighbour cells and from the culture medium (S_{self}, S_{cross} and S_{ext}, see fig. 3). These values have to be multiplied for the activity at time t, namely the drug amount in the sites of interest times the decay factor $\lambda e^{-\lambda t}$, where λ is the radioactive disintegration constant of the selected isotope. Then, d takes the form of

$$(6) \qquad d(t, z(t)) = \left[(S_{self} + S_{cross}) \frac{x_{in} - x_{eq}(z(t))}{z(t)} + S_{ext} x_{eq}(z(t)) \right] \lambda e^{-\lambda t},$$
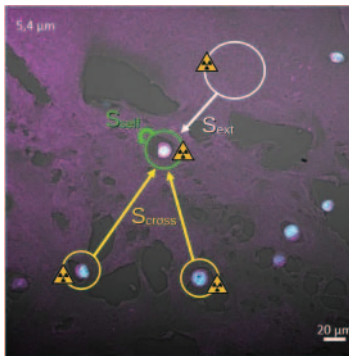

Fig. 3. – 3D cell culture with unlabeled drug (confocal microscopy) and cellular S-values.

which vanishes for $t \to \infty$ and exists $\forall z \in \mathbb{R}^+$ since

$$(7) \qquad \lim_{z \to 0} \frac{x_{\text{in}} - x_{\text{eq}}(z)}{z} = \frac{N_{\text{r}} x_{\text{in}}}{x_{\text{in}} + \beta/\alpha}.$$

Equation (6) can also express the dose-rate per cell, if the S-values consider the absorbed dose per event instead of the CLs. Finally, for the cellular growth we can employ already existing population models; for example, calling r the growth rate and K the carrying capacity of the culture, healthy cells can be expected to follow a logistic law similar to a Verhulst equation (eq. (8a)), while a Gompertzian curve (eq. (8b)) should be more appropriate to describe cancer cells [35, 36],

$$(8a) \qquad \dot{z}_0(t) = r z_0(t) \left(1 - \frac{z(t)}{K} \right),$$

$$(8b) \qquad \dot{z}_0(t) = r z_0(t) \ln \frac{z(t)}{K}.$$

In both cases we have the constraint that only $z_0(t)$ grows, but the environment is occupied by all the $z(t)$ cells. In conclusion, having applied the timescale separation for x, the following system of differential equations results (*e.g.*, for healthy cells):

$$(9) \qquad \begin{cases} \dot{z}_0(t) = r z_0(t) \left(1 - \frac{z(t)}{K} \right) - d(t, z(t)) z_0(t) + k_{\text{r}} \rho z_1(t), \\ \vdots \\ \dot{z}_n(t) = d(t, z(t)) \big(z_{n-1}(t) - z_n(t) \big) + (n+1) k_{\text{r}} \rho z_{n+1}(t) - n \rho z_n(t), \\ \vdots \\ \dot{z}_N(t) = d(t, z(t)) z_{N-1}(t) - N \rho z_N(t), \\ \dot{z}_{\text{a}}(t) = \sum_{n=1}^{N} n k_{\text{a}} \rho z_n(t) - \eta z_{\text{a}}(t). \end{cases}$$

N depends on $d(t, z(t))$ and ρ, and ideally represents the highest number of CLs that a cell can bear without one of those being repaired (or misrepaired); practically, it can be assigned *ad lib* to a compartment whose maximum is considered negligible with respect, for instance, to $z(0)$. Its existence is ensured by the following theorems.

Theorem 1 (Asymptotic behavior). *Referring to eqs. (6) and (9), $\lim_{t \to \infty} z_{n,a}(t) = 0$ and $\lim_{t \to \infty} z_0(t) = K$.*

Proof. When $t \to \infty$, $\sum_{n=1}^{N} \dot{z}_n(t) = \underline{d(t, z(t)) z_0(t)} - k_{\text{r}} \rho z_1(t) - \sum_{n=1}^{N} n k_{\text{a}} \rho z_n(t) < 0$ if $\exists n | z_n(t) > 0$, so $\sum_{n=1}^{N} z_n(t)$ decreases until $z_n(t) = 0 \ \forall n$. Similarly, $\dot{z}_{\text{a}}(t) = -\eta z_{\text{a}}(t)$, which yields $z_{\text{a}}(t) \propto e^{-\eta z_{\text{a}}(t)}$. Hence, $z_0(t)$ will become a purely logistic variable and reach K. These results still hold for $N \to \infty$. $\qquad \square$

Theorem 2 (Existence of N). *With reference to eqs. (6) and (9), the initial condition $z(0) = z_0(0) \geq 0$ implies that $\forall \varepsilon > 0 \ \exists N | z_n(t) < \varepsilon \ \forall n \geq N$.*

Proof. Due to the initial condition and the discreteness of the compartments, $z_n(t) > 0$ can be achieved only for $t \geq n \mathrm{d}t$. $\lim_{n \to \infty} n \mathrm{d}t = \infty$, thus $z_\infty(t)$ can be filled only in the $t \to \infty$ limit. However, according to theorem 1, $\lim_{t \to \infty} z_n(t) = 0$, implying also $\lim_{n \to \infty} z_n(t) = 0$. The existence of N is then guaranteed by the definition of limit. $\qquad \square$
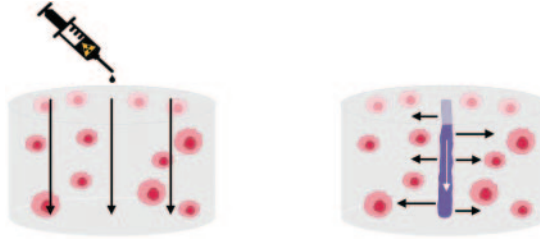
Fig. 4. – Schematic representation of a 3D cell culture in a tissue-mimicking scaffold in static (left) and dynamic (right) conditions.

2˙3. *Scaffold implementation.* – Up to now, the activity distribution has been assumed uniform in the cell culture. However, one of the strengths of this model is that it can be extended to non-uniform activity distributions, which are likely to occur in tissue-mimicking scaffolds. As a matter of fact, the radiopharmaceutical spreads in the scaffold depending on the way it is administered: in static cultures, it is injected from the top and goes down by percolation; in dynamic cultures, it flows continuously through a vessel and diffuses in the tissue (fig. 4). Such processes can be modeled with partial differential equations solvable numerically, like the diffusion equation. Those will yield the global radiopharmaceutical distribution $c(s,t)$ along a spatial coordinate s, which may represent, for instance, the height of the scaffold or the distance from the vessel: with the substitution $x_{in} \longrightarrow c(s,t)$, x_{eq} and z become functions of s as well as t. c must not depend on z or, at least, have a separable timescale; otherwise, the equation for c will have to be implemented in the system.

3. – Numerical results

Equation (9) is neither linear nor autonomous, so it can be solved only numerically. In fig. 5 an example of cell population irradiated by a targeted radioisotope is shown; $N = 2$ was selected as $z_3^{max}/z(0) \sim 10^{-4}$, however z_2 looks negligible as well. The asymptotic
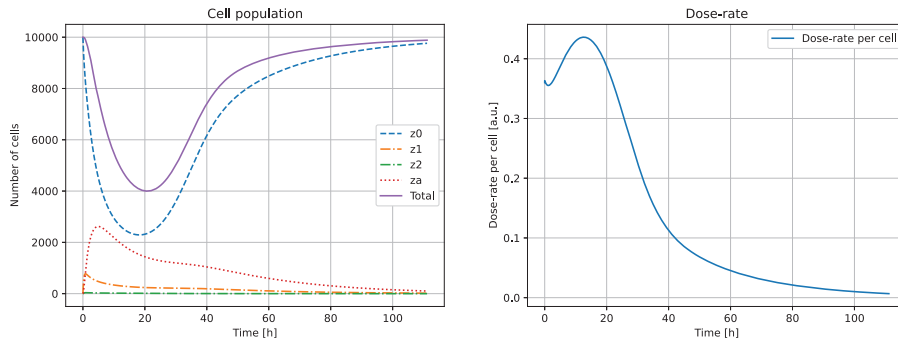

Fig. 5. – Numerical simulation with $N = 2$ cellular compartments (left) and dose-rate per cell (right) using the following parameters: $x_{in} = 10^5$, $z(0) = 10^4$, $N_r = 10^3$, $\alpha = 10^{-5}$ s^{-1}, $\beta = 10$ s^{-1}, $\lambda = 10^{-5}$ s^{-1}, $r = 10^{-4}$ s^{-1}, $K = 10^4$, $\rho = 10^{-3}$ s^{-1}, $\eta = 10^{-4}$ s^{-1}, $k_r = k_a = 0.5$, $S_{self} = 1$, $S_{cross} = 10^{-2}$, $S_{ext} = 10^{-4}$.
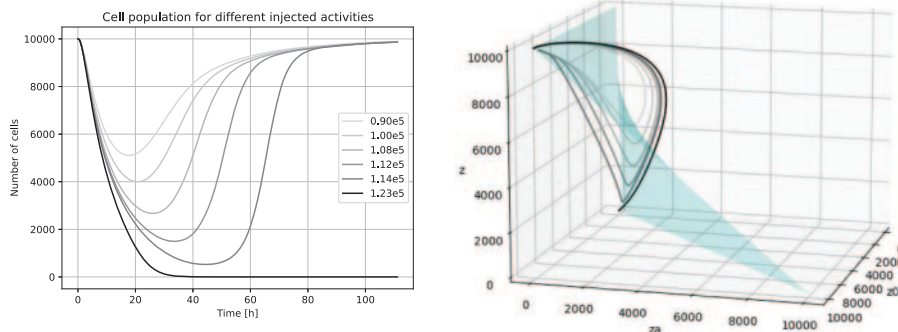
Fig. 6. – Left: numerical simulations varying x_{in} (the other parameters are the same as fig. 5); right: 3D plot in the $z_0 z_{\text{a}} z$ space, with the surface identified by eq. (10) in cyan.

behavior is the one predicted by theorem 1. The dose-rate per cell is also represented; we can notice that the shape of the decay curve varies its convexity some time after the injection: this happens because the decrease of $z(t)$ while the activity is still high implies a greater amount of bound radiopharmaceutical in each cell, maximizing the effect of the S_{self} coefficient. In this example a global maximum is visible but, increasing λ, the trend flattens out to a local maximum and then to a simple convexity.

Finally, fig. 6 shows $z(t)$ for different values of injected activity, $i.e.$, x_{in}. Due to the physical decay, if x_{in} is under a certain threshold, at a given time DNA repair and cell growth will overcome the effect of the dose-rate: $z(t)$ will touch a global minimum and grow until K is reached. On the other hand, if enough radiopharmaceutical is administered, the curve will approach zero, like the case with $x_{\text{in}} = 1.23 \times 10^5$. Actually, the model is not considering the discrete nature of the number of cells $z(t)$, thus the curve has to be forced to zero below a threshold ($e.g.$, 0.5), otherwise the population will seem to "resurrect", in agreement with theorem 1. Setting $\dot{z}(t) = 0$, it turns out that the minimum, as well as the maximum K, lies on the surface identified by

$$(10) \qquad z = K\left(1 - \frac{\eta z_{\text{a}}}{r z_0}\right).$$

4. – Conclusions

A preliminary model aimed at the support of radiobiological experiments including β-emitting radiopharmaceuticals has been built. Its main advantages, with respect to the cell population models found in the literature [20-22], are the suitability for β-emitters and the possibility to consider N subsequent CLs in each cell and non-uniform activity distributions. None of its parameters needs to be extrapolated from a cell survival curve:

- cellular S-values can be estimated via Monte Carlo simulations and validated with experimental $foci$ assays, $e.g.$, γ-H2AX;

- pharmacokinetics and cell growth parameters (α, β, r, K) can be measured in non-radioactive experiments using stable isotopes;

- the remaining biological parameters (ρ, η, k_{r}, k_{a}) can be measured in radioactive experiments, such as the $foci$ assay itself.

On the other hand, a limit of the model is certainly the fact that it can be solved only numerically; moreover, lethal aberrations coming from non-complex DNA lesions are neglected, as well as non-lethal aberrations, which can inactivate cells.

After the present work, the next steps will be for sure the measurement and/or computation of all the physical and biological parameters, a detailed study of the molecular transport in 3D scaffolds and the comparison with cell survival trials in the ADMIRAL experiment. Furthermore, other conditions of interest could be implemented; among these, we can mention the non-lethal aberrations, the coexistence of healthy and cancer cells and the inclusion of different DNA repair pathways cooperating together, in order to focus also on the low dose regime, where some pathways seem not to be triggered.

$$* * *$$

REFERENCES

[1] McMahon S. J. and Prise K. M., *Cancers*, **11** (2019) 205.
[2] McMahon S. J., *Phys. Med. Biol.*, **64** (2019) 01TR01.
[3] Solanki J. H. *et al.*, *Radiat. Res.*, **188** (2017) 221.
[4] Chatzipapas K. P. *et al.*, *Cancers*, **12** (2020) 799.
[5] Incerti S. *et al.*, *Phys. Med.*, **32** (2016) 1187.
[6] Petringa G. *et al.*, *Phys. Med.*, **58** (2019) 72.
[7] Douglass M. *et al.*, *Phys. Med. Biol.*, **60** (2015) 3236.
[8] Furuta T. and Sato T., *Radiol. Phys. Technol.*, **14** (2021) 215.
[9] Brzozowska B. *et al.*, *Front. Phys.*, **8** (2020) 567864.
[10] Ballarini F., *J. Nucleic Acids*, **2010** (2010) 350608.
[11] Ballarini F. and Carante M. P., *Radiat. Phys. Chem.*, **128** (2016) 8.
[12] Sage E. and Shikazono N., *Free Radic. Biol. Med.*, **107** (2017) 125.
[13] Sakata D. *et al.*, *Sci. Rep.*, **10** (2020) 20788.
[14] Mukherjee B. *et al.*, *Cancer Res.*, **69** (2009) 10.
[15] McMahon S. J. *et al.*, *Sci. Rep.*, **6** (2016) 33290.
[16] Stewart R. D., *Radiat. Res.*, **156** (2001) 365.
[17] Morris Z. S. *et al.*, *Semin. Radiat. Oncol.*, **31** (2020) 20.
[18] Pouget J. P. *et al.*, *Front. Med.*, **2** (2015) 12.
[19] Bannik K. *et al.*, *Sci. Rep.*, **9** (2019) 18489.
[20] Karimian A. *et al.*, *Cancer Res.*, **80** (2020) 868.
[21] Liu Z. *et al.*, *Appl. Math. Lett.*, **24** (2011) 1745.
[22] Liu Z. and Yang C., *Comput. Math. Methods Med.*, **2014** (2014) 172923.
[23] Marcatili S. *et al.*, *Phys. Med. Biol.*, **61** (2016) 6935.
[24] Palmer T. L. *et al.*, *Phys. Med. Biol.*, **66** (2021) 115023.
[25] Shinohara A. *et al.*, *Ann. Nucl. Med.*, **32** (2018) 114.
[26] Doctor A. *et al.*, *Cancers*, **12** (2020) 2765.
[27] Bielecka Z. F. *et al.*, *Biol. Rev.*, **92** (2017) 1505.
[28] Vettorato E. *et al.*, *RAD Conf. Proc.*, **6** (2022) 8.
[29] Borgna F. *et al.*, *Appl. Radiat. Isot.*, **127** (2017) 214.
[30] Verona M. *et al.*, *Molecules*, **26** (2021) 918.
[31] Benfante V. *et al.*, *J. Imaging*, **8** (2022) 92.
[32] Tosato M. *et al.*, *Molecules*, **27** (2022) 4158.
[33] Khwairakpam O. S. *et al.*, *Appl. Sci.*, **13** (2023) 309.
[34] Holland J. P. *et al.*, *Phys. Med. Biol.*, **54** (2009) 2103.
[35] Verhulst P. H., *Corresp. Math. Phys.*, **10** (1838) 113.
[36] Laird A. K., *Br. J. Cancer*, **13** (1964) 490.